Fusion of Multispectral and SAR Images by Intensity Modulation

Luciano Alparone, Luca Facheris
DET–University of Florence
Via di Santa Marta, 3
50139 Florence, Italy
alparone@lci.det.unifi.it

Stefano Baronti
IFAC–CNR
Via Panciatichi, 64
50127 Florence, Italy
s.baronti@ifac.cnr.it

Andrea Garzelli, Filippo Nencini
DII–University of Siena
Via Roma, 56
53100 Siena, Italy
garzelli@dii.unisi.it

Abstract – *This paper presents a novel multi-sensor image fusion algorithm, which extends pan-sharpening of multispectral (MS) data through intensity modulation to the integration of MS and SAR imagery. The method relies on SAR texture, extracted by ratioing the despeckled SAR image to its lowpass approximation. SAR texture is used to modulate the generalized intensity (GI) of the MS image, which is given by a linear transform extending Intensity-Hue-Saturation (IHS) transform to an arbitrary number of bands. Before modulation, the GI is enhanced by injection of highpass details extracted from the available Pan image by means of the "à-trous" wavelet decomposition. The texture-modulated pan-sharpened GI replaces the GI calculated from the resampled original MS data; then the inverse transform is applied to obtain the fusion product. Experimental results are presented on Landsat-7/ETM+ and ERS-2 images of an urban area. The results demonstrate accurate spectral preservation on vegetated regions, bare soil, and also on textured areas (buildings and road network) where SAR texture information enhances the fusion product, which can be usefully applied for both visual analysis and classification purposes.*

Keywords: Intensity-Hue-Saturation (IHS) transform, Landsat-7/Enhanced Thematic Mapper Plus (ETM+), multi-sensor data fusion, multispectral imagery, remote sensing, Synthetic Aperture Radar (SAR) imagery, texture.

1 Introduction

Multisource image fusion is one of the most complex tasks to perform integration of remote sensing image data products. One of the most relevant applications is fusion of visible-infrared (VIR) imagery with synthetic aperture radar (SAR) image data. The information contained in VIR images depends on the multispectral (MS) reflectance of the target illuminated by sunlight, whereas SAR image reflectivity mainly depends on characteristics of the surface target such as roughness and moisture, as well as on the frequency and incidence angle of the illuminating electromagnetic radiation. Although the solution may not be immediate, given the physical heterogeneity of the data, fusion of VIR and SAR image data may contribute to a better understanding of the objects observed within the imaged scene [1].

Classical approaches to multi-sensor image fusion, widely used during the past two decades, are based on modulation techniques, Principal Component Analysis (PCA), and Brovey transform [2]. Intensity modulation is generally applied to spatial enhancement of MS data: each spectral component (three channels at a time are considered as RGB components) is multiplied by the ratio of a high resolution co-registered image to the intensity component I of the MS data, where $I = (R + G + B)/3$.

An improved fusion method based on intensity modulation has been proposed by Liu [3], and tested on Landsat TM and SPOT panchromatic (Pan) data. The ratio between the higher resolution Pan and its lowpass filtered version is used to modulate the co-registered lower resolution MS image, thereby introducing spatial details, without altering its spectral properties.

When images are physically heterogeneous, different approaches are based on either decision-level fusion or multisource classifiers [4, 5]: very often the user aims at enhancing application relevant features in the fused product. Hence, application specific methods more than techniques of general use, as in the former case, have been developed [6]. The challenging task of fusion of hyperspectral and SAR imagery was recently investigated with promising result [7].

In this paper, a novel multi-sensor image fusion algorithm is presented, which extends existing solutions for pan-sharpening of MS data [3, 8], to the integration of SAR and MS+P imagery. SAR texture modulates the generalized intensity, which is obtained by applying an invertible linear transformation to the original MS data. The modulated intensity substitutes the original intensity of the MS data and the inverse linear transform is applied to obtain fused MS images.

Experimental results are presented and discussed on Landsat-7/ETM+ and ERS-2 images of an urban and suburban area. Quantitative measurements demonstrate very accurate spectral preservation on vegetated regions, bare soil, and also on textured areas (buildings and road network), where information coming from SAR enhances the fusion product, both for display and classification purposes.

The following of this paper is organized in four sections. Sect. 2 reviews the rationale of intensity modulation and points out its application to enhancement of MS bands by means of SAR texture. Sect. 3 outlines the overall fusion procedure and describes its subparts. Sect. 4 reports about experiments on Landsat-7/ETM+ and ERS-2 images taken over the city of Pavia, in Italy, and discusses results varying with work parameters. Conclusions are drawn in Sect. 5.

2 The Concept of Intensity Modulation

A desirable feature of fusion methods concerning MS images is that preservation of spectral information, regarded as changes across spectral bands, or equivalently as color hues in the composite representation of three bands at time, is guaranteed after spatial enhancement. Therefore, a variety of methods were developed based on the following steps: (a) transformation of the spectral bands, resampled at the scale of the Pan image, into Intensity-Hue-Saturation (IHS) coordinates, (b) replacement of the smooth I component with the sharp Pan image, (c) inverse transformation back to the spectral domain. IHS fusion methods [9], however, may introduce severe radiometric distortions (e.g., bias in local mean) in the sharpened MS bands, due to the lowpass component of the Pan image that affects the fused product [10]. To overcome such inconveniences, IHS fusion was extended to multiresolution (only details of I are replaced with those of Pan) [11]. IHS-based methods are straightforwardly utilized in the case of exactly three spectral bands. When a larger number of components is concerned (e.g., IKONOS and QuickBird have four spectral bands, comprising blue, green, red and near infrared (NIR)), IHS methods are applied to three band at a time, whose fusion products are displayed in color, either true or false.

Although generally labeled among methods featuring a *relative spectral contribution* [1], the Brovey transform [2], which is based on the chromaticity transform [12], practically introduced the concept of *intensity modulation* for spatial enhancement of three-band images. The Brovey transform can be expressed for *calibrated* RGB images, i.e., expressed as radiance values, by the following relationships [3]:

$$\begin{aligned} R_b &= \frac{RP}{I} \\ G_b &= \frac{GP}{I} \\ B_b &= \frac{BP}{I} \end{aligned} \tag{1}$$

in which R, G, and B are the spectral band images displayed as red, green, and blue channels, P is a higher spatial resolution image for intensity modulation, and $I = (R + G + B)/3$. All the coarser resolution data are preliminarily resampled to the finer scale of the enhancing P image, which will be the scale of the final fusion product (R_b, G_b, B_b). The Brovey transform may cause color distortion if the spectral range of the intensity replacement (or modulation) image is different from the spectral range covered by the three bands used in the color composition [2, 13, 3]. This drawback is unavoidable in color composites that do not use consecutive spectral bands. The spectral distortion introduced by these fusion techniques is uncontrolled and not easily quantifiable, because images are generally acquired by different sensors on different dates.

More recently, Liu proposed the Smoothing Filter-based Intensity Modulation (SFIM) technique [3] for sharpening of MS data by means of another image with higher spatial resolution. The fusion result is obtained as the product of the topography and texture of the higher resolution image, and of the lower resolution spectral reflectance of the original lower resolution image. The method aims at preserving the spectral characteristics of the MS image by keeping the result independent of the spectral property of the higher resolution image used for intensity modulation. This is the major advantage of SFIM over IHS and Brovey transform fusion techniques [14]. The SFIM processing formula for the case of the Landsat TM sharpening by means of a co-registered SPOT Panchromatic (P) image is the following

$$TM_i{}^{SFIM} = \frac{TM_i \cdot P}{\overline{P}} \tag{2}$$

where TM_i is the resampled i-th band of the MS image and $\overline{P}$ is the P image averaged on an $n \times n$ sliding window ($n \geq 3$). Since in the spatially enhanced spectral bands given by (2), spectral information is modulated by panchromatic texture, the author claims that the SFIM technique is not directly applicable for merging images with different illumination and imaging geometry, such as VIR and SAR. However, merging of physically different data, like VIR and thermal imagery, was previously tried by the author himself [15].

Latry *et al.* recently introduced an intensity modulation fusion algorithm for pan-sharpening of MS data from SPOT 5 [8]. After the 10m MS image (HX) is calibrated and resampled by a factor four, to obtain an HX image with 2.5m pixel size, the method consists of taking the IHS transform of the smooth 2.5m HX bands, keeping hue and saturation unchanged, and multiplying the intensity by the ratio between THR (synthesized panchromatic image at 2.5m resolution) and lowpass filtered THR, namely *soft* THR. Such a lowpass approximation of THR should have same spatial frequency content as the HX bands; hence, the intensity modulation factor differs from unity only when THR brings more spatial information than HX does. Taking the inverse IHS transform produces the final product, named THX.

Goal of this paper is to extend the concept of intensity modulation to the integration of VIR and SAR images. We propose a new fusion algorithm which integrates SAR textural features, coming mainly from built-up areas, into co-registered N-band MS images, with N arbitrary, without significantly distorting the spectral and radiometric information conveyed by VIR data.

3 Fusion Procedure

Fig. 1 illustrates the proposed multi-sensor image fusion algorithm. The input data set is composed of an amplitude SAR image, a co-registered MS image with N bands, namely $B_1, B_2, \ldots, B_N$, and a Pan image co-registered on the SAR image as well. The SAR and Pan images have spatial resolution greater than that of the MS bands. The SAR image is filtered to mitigate speckle, while preserving texture, thus obtaining the image SAR_{ds}. After despeckling, the ratio M between SAR_{ds} and its lowpass approximation, obtained by the "à-trous" wavelet algorithm as approximation at level L, is computed. The highpass details of the Pan image (level $l = 0$ of the "à-trous" wavelet transform of P) are "injected" (i.e., added) to the resampled MS

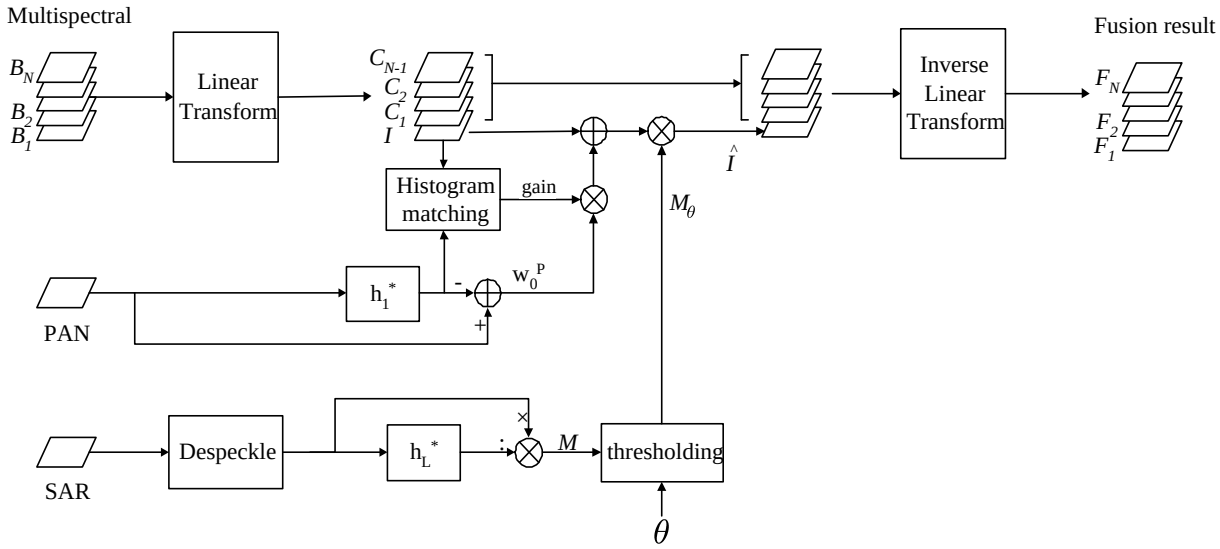

Fig. 1: Flowchart of the procedure for fusion of a low-resolution N-band MS image with a high-resolution Pan image and a high-resolution SAR image. The MS bands are preliminarily resampled at the finer scale of the fusion product by means of bicubic interpolation.

bands after equalization by a spatially constant gain term, calculated by matching the histograms of original intensity and smooth (lowpass) Pan.

3.1 "À trous" Wavelet Transform

The octave multiresolution analysis introduced by Mallat [16] for digital images does not preserve the translation invariance property. In other words, a translation of the original signal does not necessarily imply a translation of the corresponding wavelet coefficient. This property is essential in image processing. On the contrary, wavelet coefficients generated by an image discontinuity could disappear arbitrarily. This *non-stationarity* in the representation is a direct consequence of the down-sampling operation following each filtering stage.

In order to preserve the translation invariance property, the down-sampling operation is suppressed, but filters are *up-sampled* by 2^l, i.e., dilated by inserting $2^l - 1$ zeroes between any couple of consecutive coefficients. An interesting property of the undecimated domain [17] is that at the kth decomposition level, the sequences of *approximation*, $A_l(n)$, and *detail*, $W_l(n)$, coefficients are straightforwardly obtained by filtering the original signal through a bank of *equivalent filters*, given by the convolution of recursively up-sampled versions of the lowpass filter h and the highpass filter g of the analysis bank:

$$\begin{aligned} h_l^* &= \bigotimes_{m=0}^{l-1}(h \uparrow 2^m), \\ g_l^* &= \left[\bigotimes_{m=0}^{l-2}(h \uparrow 2^m)\right] \otimes (g \uparrow 2^{l-1}) \\ &= h_{l-1}^* \otimes (g \uparrow 2^{l-1}) \end{aligned} \tag{3}$$

The "à trous" wavelet transform (ATWT) [18] is an undecimated nonorthogonal multiresolution decomposition defined by a filter bank $\{h_i\}$ and $\{g_i = \delta_i - h_i\}$, with the Kronecker operator δ_i denoting an allpass filter. In the absence of decimation, the lowpass filter is up-sampled by 2^l, before processing the lth level; hence the name "à trous" which means "with holes". In two dimensions, the filter bank becomes $\{h_i h_j\}$ and $\{\delta_i \delta_j - h_i h_j\}$, which means that the 2-D detail signal is given by the pixel difference between two successive approximations, which have all the same scale 2^0, i.e., 1.

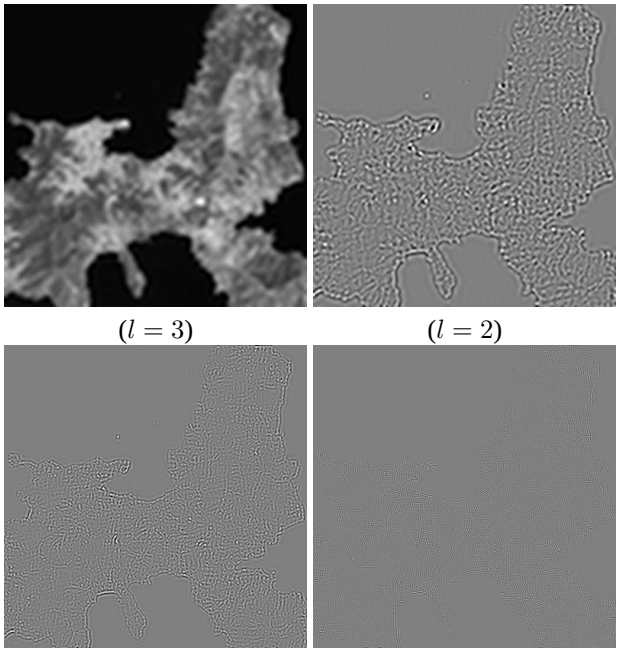

Fig. 2: "À trous" wavelet transform of Landsat-5/TM image (band # 5).

Fig. 2 portrays the ATWT of a sample image, with $L = 3$. The lth level of ATWT, $l = 1, \cdots, L$, is obtained by filtering the original image with a separable 2-D version of the lth equivalent filter (3). For a L-level decomposition, the "à trous" wavelet accommodates a number of coefficients $L + 1$ times greater than the number of pixels.

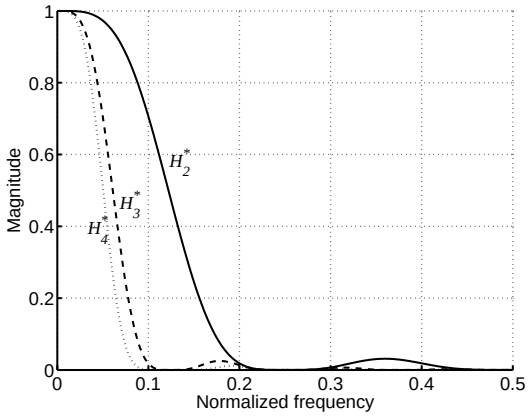

Fig. 3: Frequency responses of equivalent lowpass analysis filters of the "à trous" wavelet transform for $L = 2, 3, 4$ and prototype filter $\{h_i\} = \{-0.0313, 0, 0.2813, 0.5, 0.2813, 0, -0.0313\}$.

Due to the absence of decimation, as well as to the zero-phase and $-6\ dB$ amplitude cutoff of the filter, the synthesis is simply obtained by summing all details levels to the approximation:

$$G(i,j) = \sum_{l=0}^{L-1} W_l(i,j) + A_L(i,j) \qquad (4)$$

in which $A_L(i,j)$ and $W_l(i,j),\ l = 0, \cdots, L-1$ are obtained through 2-D separable linear convolution with h_L^* and $g_l^*,\ l = 0, \cdots, L-1$ (3), respectively. Equivalently, they can be calculated by means of a tree-split algorithm, i.e., by taking pixel differences between convolutions of the original signal with progressively up-sampled versions of the lowpass filter.

The number of decomposition levels L, which directly defines the equivalent lowpass filter h_L^*, given a half-band prototype filter $\{h_i\}$, rules the smoothness of the lowpass approximation. Fig. 3 shows the frequency responses of the equivalent filters of lowpass approximation A_L for $L = 2, 3, 4$. The frequency responses are obtained starting from a 7-tap half-band prototype filter [17].

3.2 SAR Texture Extraction

Despeckling is a key point of the fusion technique. An efficient filter for speckle removal is required to reduce the effect of the multiplicative noise on homogeneous areas, while point targets and especially textures must be carefully preserved. Thus, the ratio of despeckled SAR image to its lowpass approximation, which constitutes the modulating texture signal, is practically equal to one on areas characterized by a constant backscatter coefficient (e.g., on agricultural areas), while it significantly drifts from unity on highly textured regions (urban and built-up areas) [19]. In such regions intensity modulation is particularly effective: spatial features that are detectable in the SAR image only can be properly introduced by the fusion procedure into the VIR image, without degrading its spectral signatures and radiometric accuracy, to provide complementary information.

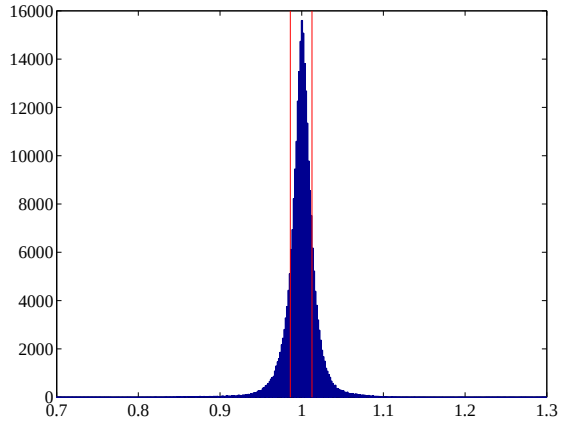

Fig. 4: Histogram of modulating SAR texture: threshold $\theta = \sigma_t$ is highlighted.

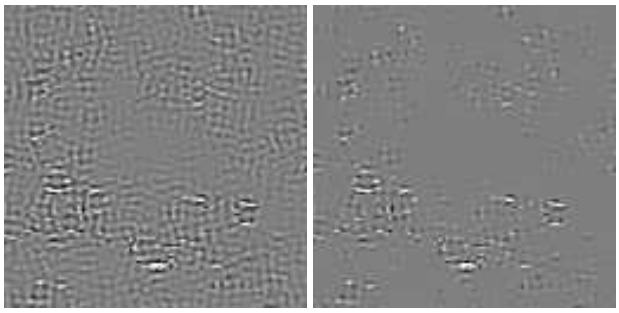

(a) (b)

Fig. 5: Modulating SAR texture (a) before and (b) after soft-thresholding.

Due to unbiasedness of despeckling performed in the undecimated wavelet domain without resorting to logarithm [20, 21], the ratio image $M = SAR_{ds}/(SAR_{ds} \otimes h_L^*)$ has unity mean value, as shown in Fig. 4. Spurious fluctuations in homogeneous areas around the mean value $m = 1$, due to imperfect despeckling, intrinsic signal variability of rough surfaces, and instability of image ratioing, are clearly visible in Fig. 5(a).

By denoting with σ_t the standard deviation of the distribution of the modulating SAR texture M, a soft thresholding with threshold $\theta = k \cdot \sigma_t$ is applied to M: values outside the interval $[1 - k\sigma_t, 1 + k\sigma_t]$ are diminished in modulus by $k\sigma_t$ and retained, while values lying within this interval are set to the mean value $\mu_t \approx 1$ (see Fig. 4). The resulting texture map M_θ, shown in Fig. 5(b), contains spatial features which are easily detected by SAR and can be properly integrated into the MS image data by modulating the intensity of the MS image.

3.3 Generalized I-H-S Transform

Any linear combination of N spectral bands $B_1, B_2, \ldots, B_N$, with weights summing to unity, may be taken in principle as a generalization of intensity [10]. If a Pan image is available to enhance spatial resolution, taking into account of the N correlation coefficients between resampled MS bands and Pan image, $\rho_{i,P}$, yields the generalized intensity (GI) as $\mathcal{I} = \sum_i \alpha_i \cdot B_i$, in which $\alpha_i = \rho_{i,P}/(\sum_i \rho_{i,P})$. A linear transformation T to be

(a) (b)

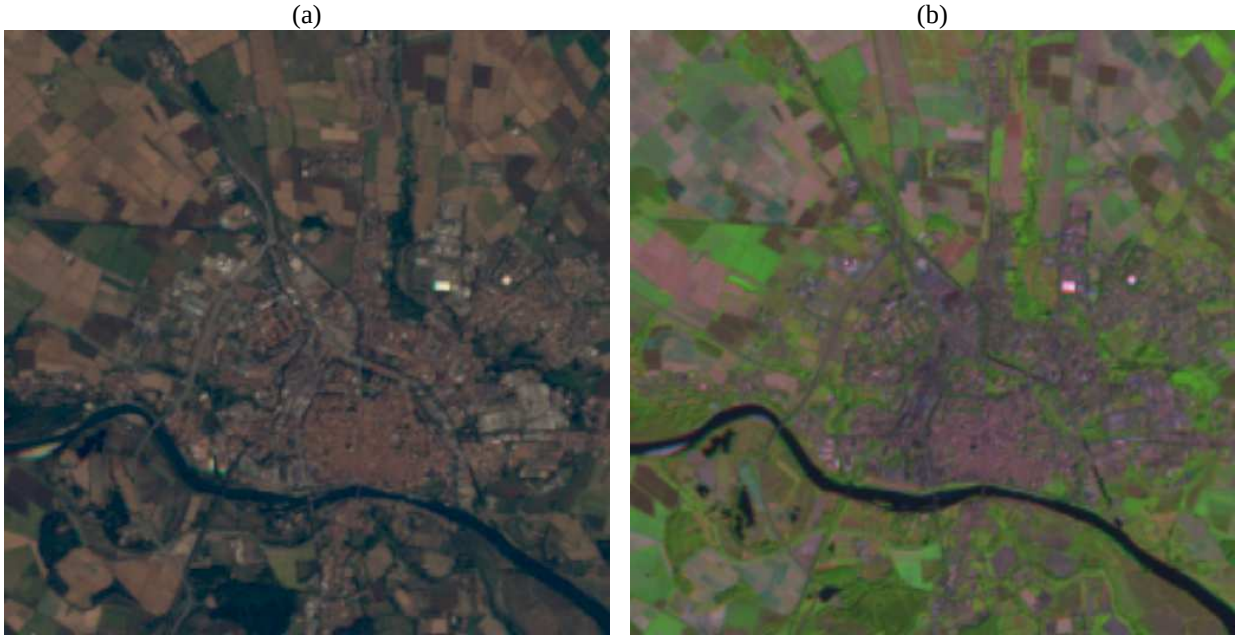

(a) (b)

Fig. 6: Original data set of the city of Pavia (all optical data resampled to the 12.5m scale of geocoded ERS): (a) ERS-2 SAR (3-looks amplitude); (b) Landsat-7/ETM+ Panchromatic; (c) Landsat-7/ETM+ true color (RGB composition of 3-2-1); (d) Landsat-7/ETM+ false color (RGB composition of 5-4-3).

applied to the original MS pixel vectors is given by:

$$\mathbf{T} = \begin{pmatrix} \alpha_1 & \alpha_2 & \alpha_3 & \alpha_4 & \dots & \alpha_N \\ 1/2 & -1/2 & 0 & 0 & \dots & 0 \\ 0 & 1/2 & -1/2 & 0 & \dots & 0 \\ 0 & 0 & 1/2 & -1/2 & \dots & 0 \\ & & & \ddots & & \\ 0 & 0 & \dots & 0 & 1/2 & -1/2 \end{pmatrix} \tag{5}$$

If all the α_is are nonzero, (5) is nonsingular and hence invertible. The generalized IHS transform yields the GI, $\mathcal{I}$, and $N-1$ generalized spectral differences, C_n, encapsulating the spectral information. If T is applied to an N-band image, with N arbitrary, and the $\mathcal{I}$ component only is manipulated, e.g., sharpened by Pan details and modulated by SAR texture, the spectral information of the original MS data set is preserved, once the modulated GI $\hat{\mathcal{I}}$ substitutes the original GI $\mathcal{I}$ and the inverse transform T^{-1} is applied to obtain the fused MS image, as shown in Fig. 1.

4 Experimental Results

The proposed fusion method has been tested on an ERS-2 SAR image of the city of Pavia (Italy), acquired on October 28, 2000, and on a Landsat-7/ETM+ image, with 30m bands (1, 2, 3, 4, 5, and 7), acquired on September 22, 2000, together with the 15m Pan image. All the optical data have been manually co-registered to the ERS image, which is geocoded with $12.5 \times 12.5m^2$ pixel size. The absence of

(a) (b)

Fig. 7: ETM+ and ERS fusion with $L = 3$ and $k = 1.25$: (a) 3-2-1 true color composite; (b) 5-4-3 false color composite.

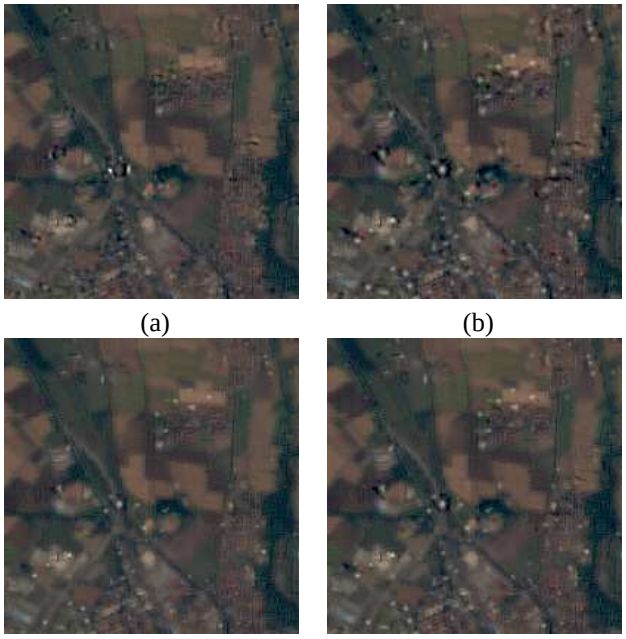

(a) (b)

(c) (d)

Fig. 8: True color 200×200 details of fusion products. (a): $L = 2$ and $k = 1$; (b): $L = 3$ and $k = 1$; (c): $L = 2$ and $k = 1.5$; (d): $L = 3$ and $k = 1.5$.

significant terrain relief would make automated registration possible, by resorting to suitable modeling of acquisition geometries of optical and SAR platforms [22]. Fig. 6 shows 512×512 details at 12.5m pixel size. Figs. 6(c) and 6(d) display true (bands 3-2-1 as R-G-B) and false (bands 5-4-3 as R-G-B) color composites.

Fig. 7 shows 512×512 fusion results as true and false color composites, respectively. Urban and built-up areas, as well as roads and railway are clearly enhanced; an almost perfect preservation of spectral signatures is visible from comparisons with Figs. 6(c) and 6(d).

To provide a deeper insight of the two parameters, i.e., approximation depth L driving the coarseness of SAR texture and constant k tuning soft thresholding, which rule modulation of GI by SAR texture, different fusion results are reported in Fig. 8 for a 200×200 image fragment. Three values of L ($L = 2, 3, 4$) and four thresholds, i.e., $\theta = k \cdot \sigma_t$, with $k = 0, 1, 2, 3$, have been considered ($k = 0$ indicates absence of thresholding). The most noteworthy fusion results are illustrated in Fig. 8. For the case study of Fig. 7, the choice $L = 3$ and $k = 1.25$ seems to provide the best tradeoff between visual enhancement and accurate integration of SAR features in MS bands. However, the choice of the parameters L and k ($1 \leq k \leq 2$ with either $L = 2$ or $L = 3$, for best results) reasonably depends on both landscape and applications. How the spectral information of the original MS image is preserved is demonstrated by the values of average Spectral Angle Mapper (SAM) reported in Table 1. If $\mathbf{v} = \{v_1, v_2, \cdots, v_N\}$ denotes the original spectral vector of a pixel and $\hat{\mathbf{v}} = \{\hat{v}_1, \hat{v}_2, \cdots, \hat{v}_N\}$ the distorted vector obtained after fusion, SAM is defined as the absolute angle between the two vectors:

$$SAM(\mathbf{v}, \hat{\mathbf{v}}) = \arccos\left(\frac{< \mathbf{v}, \hat{\mathbf{v}} >}{||\mathbf{v}||_2 \cdot ||\hat{\mathbf{v}}||_2}\right). \qquad (6)$$

Table 1: Spectral distortion (average SAM) between resampled original and fused MS pixels) vs. approximation level L, and soft threshold of modulating texture, $\theta = k\sigma_t$.

	$k = 0$	$k = 1$	$k = 2$	$k = 3$
$L = 2$	1.102°	0.510°	0.413°	0.395°
$L = 3$	2.123°	0.672°	0.439°	0.405°
$L = 4$	2.777°	0.720°	0.449°	0.415°

As it appears, increasing L and/or decreasing k may cause overenhancement, which is accompanied by a loss

of spectral fidelity in the fusion product. This effect is particularly evident when soft-thresholding of SAR texture is missing ($k = 0$). An analogous trend was found for the differences between mean of original and fused bands. However, the highpass nature of the enhancing contributions from Pan and SAR makes radiometric distortion, i.e., mean bias, to be negligibly small in all cases.

5 Conclusions

Intensity modulation has proven itself to be promising for multi-sensor image fusion of SAR and multiband optical data. The proposed fusion procedure allows homogenous data (MS and Pan) to be effectively integrated with the physically heterogeneous SAR backscatter. The method does not directly merge spectral radiances and SAR reflectivity; instead, the combination is obtained by modulating the intensity of MS bands, after sharpening by injection of Pan highpass details, through texture extracted from SAR. An arbitrary number of spectral bands can be dealt with, thanks to the definition a generalized intensity, tailored to the spectral correlation of MS and Pan data.

Experiments carried out on Landsat-7/ETM+ and ERS data of an urban area demonstrate careful preservation of spectral signatures on vegetated regions, bare soil, and also on built-up areas (buildings and road network) where information from SAR texture enhances the fusion product both for visual analysis and classification purposes. Objective evaluations of the quality of fusion results are presented as spectral fidelity scores with the original MS data. Future work will concern measurements of classification accuracy, obtained either with or without fusion, to demonstrate its benefits for practical applications.

Acknowledgment

The authors are grateful to Fabio Dell'Acqua and Paolo Gamba from the University of Pavia for providing the ETM+ and ERS-2 data, and to Fabrizio Argenti from the University of Florence for the code of speckle filter [20].

References

[1] C. Pohl and J. L. van Genderen. Multisensor image fusion in remote sensing: concepts, methods, and applications. *Int. J. Remote Sensing*, 19(5):823–854, 1998.

[2] P. S. Chavez, S. C. Sides, and J. A. Anderson. Comparison of three different methods to merge multiresolution and multispectral data: Landsat TM and SPOT panchromatic. *Photogram. Engin. Remote Sensing*, 57(3):295–303, 1991.

[3] J. Liu. Smoothing filter-based intensity modulation: a spectral preserve image fusion technique for improving spatial details. *Int. J. Remote Sensing*, 21(18):3461–3472, 2000.

[4] A. H. Schistad Solberg, T. Taxt, and A. K. Jain. A Markov random field model for classification of multisource satellite imagery. *IEEE Trans. Geosci. Remote Sensing*, 34(1):100–113, Jan. 1996.

[5] A. H. Schistad Solberg, A. K. Jain, and T. Taxt. Multisource classification of remotely sensed data: fusion of Landsat TM and SAR images. *IEEE Trans. Geosci. Remote Sensing*, 32(4):768–778, July 1994.

[6] M. Moghaddam, J. L. Dungan, and S. Acker. Forest variable estimation from fusion of SAR and multispectral optical data. *IEEE Trans. Geosci. Remote Sensing*, 40(10):2176–2187, Oct. 2002.

[7] C.-M. Chen, G. F. Hepner, and R. R. Forster. Fusion of hyperspectral and radar data using the IHS transformation to enhance urban surface features. *ISPRS J. Photogramm. Remote Sensing*, 58(1-2):19–30, June 2003.

[8] C. Latry, H. Vadon, M. J. Lefèvre, and H. De Boissezon. SPOT5 THX: a 2.5m fused product. In *Proc. 2nd GRSS/ISPRS Joint Workshop on Remote Sensing and Data Fusion over Urban Areas*, pages 87–89, 2003.

[9] W. Carper, T. Lillesand, and R. Kiefer. The use of Intensity-Hue-Saturation transformations for merging SPOT panchromatic and multispectral image data. *Photogram. Engin. Remote Sensing*, 56(4):459–467, 1990.

[10] T.-M. Tu, S.-C. Su, H.-C. Shyu, and P. S. Huang. A new look at IHS-like image fusion methods. *Information Fusion*, 2(3):177–186, Sep. 2001.

[11] J. Núñez, X. Otazu, O. Fors, A. Prades, V. Palà, and R. Arbiol. Multiresolution-based image fusion with additive wavelet decomposition. *IEEE Trans. Geosci. Remote Sensing*, 37(3):1204–1211, May 1999.

[12] A. R. Gillespie, A. B. Kahle, and R. E. Walker. Color enhancement of highly correlated images–II. Channel ratio and chromaticity transformation techniques. *Remote Sens. Environ.*, 22(2):343–365, 1987.

[13] J. G. Liu, J. McM. Moore, and J. D. Haigh. Simulated reflectance technique for ATM image enhancement. *Int. J. Remote Sensing*, 18(2):243–254, 1997.

[14] J. Harris, R. Murray, and T. Hirose. IHS transform for the integration of radar imagery with other remotely sensed data. *Photogram. Engin. Remote Sensing*, 56(10):1631–1641, 1990.

[15] J. G. Liu and J. McM. Moore. Pixel block intensity modulation: adding spatial detail to TM band 6 thermal imagery. *Int. J. Remote Sensing*, 19(12):2477–2491, 1998.

[16] S. Mallat. A theory for multiresolution signal decomposition: the wavelet representation. *IEEE Trans. Pattern Anal. Machine Intell.*, PAMI-11(7):674–693, July 1989.

[17] B. Aiazzi, L. Alparone, S. Baronti, and A. Garzelli. Context-driven fusion of high spatial and spectral resolution data based on oversampled multiresolution analysis. *IEEE Trans. Geosci. Remote Sensing*, 40(10):2300–2312, Oct. 2002.

[18] P. Dutilleux. An implementation of the "algorithme à trous" to compute the wavelet transform. In J. M. Combes, A. Grossman, and Ph. Tchamitchian, editors, *Wavelets: Time-Frequency Methods and Phase Space*, pages 298–304. Springer, Berlin, 1989.

[19] F. T. Ulaby, F. Kouyate, B. Brisco, and T. H. Lee Williams. Textural information in SAR images. *IEEE Trans. Geosci. Remote Sensing*, 24(2):235–245, Mar. 1986.

[20] F. Argenti and L. Alparone. Speckle removal from SAR images in the undecimated wavelet domain. *IEEE Trans. Geosci. Remote Sensing*, 40(11):2363–2374, Nov. 2002.

[21] H. Xie, L. E. Pierce, and F. T. Ulaby. Statistical properties of logarithmically transformed speckle. *IEEE Trans. Geosci. Remote Sensing*, 40(3):721–727, Mar. 2002.

[22] P. Dare and I. Dowman. An improved model for automatic feature-based registration of SAR and SPOT images. *ISPRS J. Photogramm. Remote Sensing*, 56(1):13–28, 2003.